Jpn. J. Appl. Phys, 53(2S), 02BB03 (2014)

Enhancement of Ultraviolet Light Responsivity of a Pentacene Phototransistor by Introducing Photoactive Molecules into a Gate Dielectric

Toan Thanh Dao[1,2], Toshinori Matsushima[1], Motonobu Murakami[3,4], Kei Ohkubo[3,4], Shunichi Fukuzumi[3,4,5], and Hideyuki Murata[1*]

[1]Japan Advanced Institute of Science and Technology, Nomi, Ishikawa 923-1292, Japan

[2]University of Transport and Communications, Dong Da, Hanoi, Vietnam

[3]Department of Material and Life Science, Graduate School of Engineering, Osaka University

[4]ALCA, Japan Science and Technology Agency (JST), Suita, Osaka 565-0871, Japan

[5]Department of Bioinspired Science, Ewha Womans University, Seoul 120-750, Korea

**E-mail address*: murata-h@jaist.ac.jp

ABSTRACT

We demonstrated a new approach to fabricate an ultraviolet (UV) photodetector with a pentacene transistor structure where photoactive molecules of 6-[4′-(*N*,*N*-diphenylamino)phenyl]-3-ethoxycarbonylcoumarin (DPA-CM) were introduced into a poly(methyl methacrylate) (PMMA) gate dielectric. DPA-CM molecules strongly absorb UV light and form stable charge-separation states. When a negative gate voltage was scanned to a gate electrode of the transistor, the charge-separation states of DPA-CM molecules were converted into free electrons and holes. The free electrons traversed and subsequently reached an interface of the PMMA:DPA-CM layer and a polystyrene buffer layer, inducing accumulation of additional holes in a pentacene channel. Therefore, under 2.54 mW/cm^2 of 365 nm UV irradiation, a marked increase in drain current by 6.1×10^2 times were obtained from the transistor. Moreover, the phototransistor exhibited a high light responsivity of 0.12 A/W which is about one order of magnitude larger than that of a conventional pentacene phototransistor [Lucas et al., Thin Solid Films **517** (2009) 280]. This result will be useful for manufacturing of a high-performance UV photodetector.

1. Introduction

An ultraviolet (UV) photodetector is a key component used for various applications in a medical instrument, a sterilization monitor, a fire alarm system, a solar UV radiation monitor and an ozone sensor.[1–5] Recently, photodetectors based on organic materials have gained considerable attention[6] because of their unique and attractive features including low-cost, simple fabrication, low temperature manufacturing, and mechanical flexiblility which make it possible to manufacture flexible, foldable, and large-area devices for modern electronics.[7–11] Resistor,[12] diode,[13] and transistor[14] structures have been utilized as photodetectors. Among these organic photodetectors, the phototransistor is promising because it functions both light detection and signal amplification so that it allows sensing a small level of light intensity.[2]

Light responsivity, *R*, defined as a ratio of a photo drain current to incident light intensity, is one of the most important parameters in the phototransistor.[6] Under light irradiation, electron-hole pairs are formed by photon absorption of a semiconductor channel material. When an external voltage is applied to the electrodes, the electron-hole pairs are separated into free charges and result in an increase in drain current. Thus, the *R* depends on matching the absorption wavelength of the semiconducting material with the light wavelength. Although pentacene is widely used as a semiconducting layer of visible phototransistors,[15–25] the *R* of the pentacene phototransistor is low in the UV light region due to poor UV light absorption by pentacene.[26–30]

In the present work, we demonstrate significant improvement of *R* in a pentacene phototransistor by introducing a photoactive gate dielectric layer composed of the layers of 6-[4′-(*N*,*N*-diphenylamino)phenyl]-3-ethoxycarbonylcoumarin (DPA-CM) doped into

poly(methyl methacrylate) (PMMA) (PMMA:DPA-CM) and polystyrene. DPA-CM molecules strongly absorb UV light and form stable charge-separation states. When a negative gate voltage is applied to the gate dielectric, the charge-separation states of DPA-CM molecules are converted into free electrons and holes. The free electrons accumulated at the interface of PMMA:DPA-CM/polystyrene induce additional hole accumulation in a pentacene channel, resulting in one order of magnitude larger *R* value when compared with the conventional pentacene phototransistors previously reported.[28)]

2. Experimental Methods

Figures 1(a) and 1(b) show the cross section of the top-contact pentacene phototransistor and the chemical structures of pentacene and DPA-CM, respectively. Glass substrates coated with a 150 nm gate electrode layer of indium tin oxide (ITO) were cleaned using ultrasonication, followed by UV-O_3 treatment. The synthetic method and material characterization of DPA-CM were reported in Ref. 31. PMMA (Aldrich, M_w = 97,000) and DPA-CM with a 10:1 molar ratio of a monomer unit of PMMA to DPA-CM were dissolved in chloroform (the concentration of PMMA was 2 wt %). A 263-nm-thick layer of the PMMA:DPA-CM composite was prepared on the ITO by spin-coating of the solution at 2000 rpm for 60 s, and heated on a hot plate at 100 ^oC for 60 min to remove the residual solvent. Then, a 67-nm-thick polystyrene (Aldrich, M_w = 280,000) buffer layer was formed onto the PMMA:DPA-CM layer by spin-coating of a m-xylene solution (1 wt%) at 1000 rpm for 60 s and dried at 100 ^oC for 60 min. We used m-xylene because the underlying PMMA:DPA-CM layer is insoluble in m-xylene. A 30-nm-thick layer of pentacene (Aldrich, purified by vacuum sublimation twice) was formed on the polystyrene buffer layer by conventional vacuum

deposition at a deposition rate of 0.02 nm s^{-1}. Finally, the device was completed by deposition of gold source-drain electrodes (50 nm) at a deposition rate of 0.03 nm s^{-1} through a shadow mask. The length (L) and width (W) of the channel were 50 and 2000 μm, respectively. The vacuum deposition processes were carried out at a pressure of 2×10^{-6} Torr.

To estimate the thickness of each layer in the double-layer gate dielectric of PMMA:DPA-CM and polystyrene, we used the capacitance measurement. For instance, the double-layer dielectric capacitor can be regarded as a serial connection of two capacitors as shown in Fig. 1(c). Thus, the capacitance per unit area (C_i) of the double-layer dielectric capacitor can be expressed as

$$C_i = \frac{\varepsilon_0 \varepsilon_{r,1} \varepsilon_{r,2}}{d_1 \varepsilon_{r,2} + d_2 \varepsilon_{r,1}}, \qquad (1)$$

where ε_0 is the vacuum permittivity (8.854×10^{-12} F/m), $\varepsilon_{r,1}$ and $\varepsilon_{r,2}$ are the dielectric constants of polystyrene and PMMA:DPA-CM, and d_1 and d_2 are the thickness of the polystyrene and PMMA:DPA-CM layers in the double-layer structure. On the other hand, the thickness of the double-layer structure (d) consists of the d_1 and d_2:

$$d = d_1 + d_2. \qquad (2)$$

The C_i, $\varepsilon_{r,1}$ and $\varepsilon_{r,2}$ were determined to be 65.4 pF/mm^2, 2.6 and 2.4, respectively, with an Agilent 4284A LCR meter at 1 kHz. The d was measured to be 330 nm by scratching the film and measuring a height difference across the scratch with an atomic force microscope (Keyence VN-8000). By solving Eqs. (1) and (2), the d_1 and d_2 were found to be ~67 and ~263 nm, respectively.

Electrical measurements of the phototransistor were done at room temperature using a Keithley 4200 semiconductor characterization system in a dry nitrogen atmosphere. 365 nm UV light generated from an Omron ZUV UV irradiator was irradiated from a glass substrate side as illustrated in Fig. 1(a). The UV light intensity was measured by a Coherent FieldMax II-TO laser power meter.

3. Results and Discussion

3.1. Performances of phototransistor

Figure 2 presents the electrical characteristics of the pentacene phototransistor under dark. In the output characteristics, the drain current (I_D) clearly demonstrates linear and saturation regions under a negative gate voltage (V_G), suggesting the standard p-type field-effect operation [Fig. 2(a)]. The saturation-region hole mobility (μ) is estimated by fitting the plot of the square root of I_D versus V_G with an equation:[32)]

$$I_D = \frac{WC_i}{2L}\mu(V_G - V_{th})^2, \qquad (3)$$

where V_{th} is the threshold voltage. The V_{th}, on/off current ratio, and μ estimated from the transfer characteristics shown in Fig. 2(b) are –3.7 V, 3.8×10^5, and 0.02 $cm^2\ V^{-1}\ s^{-1}$, respectively. The transistor performances are similar to those observed from previous pentacene phototransistors.[24–30)]

The photoelectrical characteristics of the phototransistor are shown in Fig. 3(a). The transfer curve shifted to a high I_D under 2.54 mW/cm^2 of UV light, resulting in a change in V_{th} (ΔV_{th}) of 2.1 V. The maximum ratio of I_D under light to I_D under dark was 6.1×10^2 at V_G = –2 V. The slight increase in gate-leakage current (I_G) of the phototransistor under the UV light irradiation [Fig. 3(a)] is on the order of 10^{-9} A which

is negligible contribution to the increase in I_D. After turning off the UV light, the transfer curve was measured again immediately. As indicated by the open triangles in Fig. 3(a), the transfer curve almost returned to the initial position, indicating that the transfer curve shift originates from the UV light irradiation. We confirmed that the transfer curves shifts were repeatable for many cycles, suggesting that our phototransistor has a potential to work as a stable UV photodetector.

The R of the phototransistor is evaluated utilizing the following equation:[6)]

$$R = \frac{I_{D,ph}}{P_{inc}} = \frac{I_{D,ill} - I_{D,dark}}{EA}, \qquad (4)$$

where $I_{D,ph}$ is the I_D generated by the light illumination, P_{inc} is the incident light intensity, $I_{D,ill}$ and $I_{D,dark}$ are the I_D under light illumination and dark, respectively, E is the incident light intensity per unit area, and A is the area of the transistor channel. Figure 3(b) shows the relationship between the estimated R and the V_G under 2.54 mW/cm^2 of the UV light intensity. The R was found to increase as increasing the V_G. On other aspect, we have investigated the UV light intensity dependence of the R. As shown in Fig. 3(c), the R decreased as increasing the light intensity. This tendency is similar to the experimental results reported by other groups.[23,24,33)] The maximum R (R_{max}) was obtained to be 0.12 A/W which is about one order of magnitude higher than that in previously reported UV pentacene phototransistors.[28,29)] In addition, this value was obtained at the V_G of −18 V which is the lowest V_G among previous works.[16–30)]

3.2. Operation mechanism

To clarify the working mechanism of the phototransisor, a transistor device without DPA-CM [glass substrate/ITO (150 nm)/PMMA (263 nm)/polystyrene (67

nm)/petancene (30 nm)/Au (50 nm)] was constructed with the same preparation condition. Figure 4 (a) shows the transfer curves of the device were measured during irradiating 2.54 mW/cm^2 of the UV light from the bottom glass substrate side or the top pentacene side. The transfer curves of the device without DPA-CM are almost unchanged even under the UV light illumination and independent of the illumination directions. Based on the experimental data shown in Fig. 4(a), we have calculated the R and ΔV_{th} of the device without DPA-CM, i.e., $R_{max} = 3.23\times10^{-4}$ A/W and $\Delta V_{th} = 0.01$ V for the bottom illumination and $R_{max} = 3.82\times10^{-4}$ A/W and $\Delta V_{th} = 0.35$ V for the top illumination. The R values are about three orders of magnitude smaller than those of the device with DPA-CM.

Figure 4(b) shows the UV-vis absorption spectra of a 30-nm-thick pentacene film (black curve) and a 263-nm-thick PMMA:DPA-CM film (red curve), which were measured with a JASCO V-570 spectrometer. Since the absorbance of pentacene at 365 nm is very weak,[27,29] a photocurrent originating from direct carrier generation in pentacene is very small, resulting in the unchanged and independent transfer curves [Fig. 4(a)]. On the other hand, the absorbance of PMMA:DPA-CM is much stronger than that of pentacene in the UV region, suggesting that DPA-CM plays an essential role in inducing the transfer curve shift.

Under the UV light (365 nm), singlet and then triplet states of DPA–CM are generated and then converted into a charge-separation state,[31] the charge-separation state is easily converted into free carriers by an external electric field. In order to verify this hypothesis, a photoactive dielectric device with a structure of glass/ITO/PMMA:DPA-CM/Au [Fig. 5(a)] was fabricated. Current versus UV light intensity at different voltages of the device was characterized. As shown in Fig. 5(b),

the current increased with increasing the UV light intensity and voltage, indicating the photocharge generation inside the PMMA:DPA-CM film.

The *R* of the photoactive dielectric device was also estimated by dividing the photocurrent by the incident light intensity. As can be seen in Fig. 5(c), the *R* of the photoactive dielectric device is changed in the manner similar to that of the phototransistor [Fig. 3(c)]. The decrease in the *R* observed from Figs. 3(c) and 5(c) at the high UV light intensity is speculated to be because more photogenerated charges inside the PMMA:DPA-CM layer are created as well as the recombination of the photogenerated charges increases. However, the *R* of the phototransistor is larger than that of the photoactive dielectric device thanks to the signal amplification ability of the transistor structure.[33)]

There is a possibility that the transfer curve shift originates from the dipole polarization of the gate dielectric. In that case, a change of capacitance of the gate dielectric should be observed. However, we confirmed that the gate dielectric capacitance under UV light irradiation (C_i = 65.4 pF/mm^2) is the same as that under dark (C_i = 65.4 pF/mm^2). Based on the experimental results shown in Fig. 5, we illustrate the operation principle of the phototransistor in Fig. 6. Under dark, the double-layer gate dielectric acts as a normal insulating layer for field-effect operation and hole accumulation in the transistor channel is inducted by the gate electric field only [Fig. 6(a)]. When the UV light is irradiated to the phototransistor, the charge-separation state is generated. Upon application of a voltage between the gate and drain electrodes, the charge-separation state is converted into free electrons and holes. Under the gate electric field, the photogenerated holes move to the ITO gate electrode and the photogenerated electrons move to the interface of the PMMA:DPA-CM layer and the polystyrene buffer

layer [Fig. 6(b)]. The role of the polystyrene buffer layer is to block the photogenerated electrons.[34] We confirmed that the layers of PMMA:DPA-CM and polystyrene had the same surface morphologies and surface morphologies of the overlaying pentacene layers were unchanged as well. The additional electric field created by the photogenerated electrons further induces additional accumulation of holes in the pentacene channel. As the consequence, the concentration of holes in the channel becomes larger than that of the device in dark, leading to the positive shift of the transfer curve [filled circles in Fig. 3(a)]. We would like to emphasize that the mechanism of our phototransistor proposed here is different from conventional phototransistors[15–30] where the I_D is increased by photocharges generated in the transistor channel via the direct photoexcitation of pentacene.

4. Conclusions

We have demonstrated a new method to realize a pentacene UV phototransistor using photoactive molecules of DPA-CM. DPA-CM acts as a sensing material thanks to its strong absorption in an UV region and a stable charge-separation state. A hole concentration in the pentacene channel was enhanced by an additional electric field created by photogenerated electrons that were accumulated at the PMMA:DPA-CM/polystyrene buffer layer interface. The phototransistor exhibited a high responsivity of 0.12 A/W under UV irradiation of 365 nm which is one order of magnitude larger than that of conventional pentacene phototransistors. We suggest that the above-mentioned results are useful to fabricate a high-performance UV photodetector.

Acknowledgements

The authors thank Dr. Heisuke Sakai (Flexible Electronics Research Center, AIST) for fruitful discussion. This work was partially supported by a Grant-in-Aid for Scientific Research (Grant No. 20241034) and Scientific Research on Innovative Areas “pi-Space” (Grant No. 20108012) from the Ministry of Education, Culture, Sports, Science, and Technology.

1) G. Chai , O. Lupan , L. Chow, and H. Heinrich: Sens. Actuators A **150** (2009) 184.

2) Osinsky, S. Gangopadhyay, R. Gaska, B. Williams, M. A. Khan, D. Kuksenkov, and H. Temkin: Appl. Phys. Lett. **71** (1997) 2334.

3) C. A. Smith, H. W. H. Lee, V. J. Leppert, and S. H. Risbud: Appl. Phys. Lett. **75** (1999) 1688.

4) J. H. He, Y. H. Lin, M. E. McConney, V. V. Tsukruk, Z. L. Wang, and G. Bao: J. Appl. Phys. **102** (2007) 084303.

5) A. J. Gimenez, J. M. Yanez-Limon, and J. M. Seminario: IEEE Sens. J. **13** (2013) 1301.

6) K.-J. Baeg, M. Binda, D. Natali, M. Caironi, and Y.-Y. Noh: Adv. Mater. **25** (2013) 4267.

7) T. Sekitani and T. Someya: Jpn. J. Appl. Phys. **51** (2012) 100001.

8) T. T. Dao, T. Matsushima, and H. Murata: Org. Electron. **13** (2012) 2709.

9) M. W. Alam, Z. Wang, S. Naka, and H. Okada: Jpn. J. Appl. Phys. **52** (2013) 03BB08.

10) Y. Fukaya, A. Inoue, Y. Fukunishi, S. Hotta, and T. Yamao: Jpn. J. Appl. Phys. **52** (2013) 05DC09.

11) T. T. Dao, T. Matsushima, R. Friedlein, and H. Murata: Org. Electron. **14** (2013) 2007.

12) G. Dong, Y. Hu, C. Jiang, L. Wang, and Y. Qiu: Appl. Phys. Lett. **88**, (2006) 051110.

13) X. Gong, M. Tong, Y. Xia, W. Cai, J. S. Moon, Y. Cao, G. Yu, C.-L. Shieh, B. Nilsson, and A. J. Heeger: Science **325** (2009) 1665.

14) J. Park, D. W. Kim, B. K. Lee, and Y.-S. Jeong, M. Petty, J. S. Choi, and L.-M. Do: Jpn. J. Appl. Phys. **52** (2013) 05DC12.

15) Y. Hu, G. Dong, L. Wang, and Y. Qiu: Jpn. J. Appl. Phys. **45** (2006) L96.

16) H.-W. Zan, S.-C. Kao, and S.-R. Ouyang: IEEE Electron Device Lett. **31** (2010) 135.

17) Y. Hu, G. F. Dong, C. Liu, L. D. Wang, and Y. Qiu: Appl. Phys. Lett. **89** (2006) 072108.

18) S. Okur, F. Yakuphanoglu, and E. Stathatos: Microelectron. Eng. **87** (2010) 635.

19) J.-H. Kwon, M.-H. Chung, T.-Y. Oh, H.-S. Bae, J.-H. Park, B.-K. Ju, and F. Yakuphanoglu: Sens. Actuators A **156** (2009) 312.

20) M. Debucquoy, S. Verlaak, S. Steudel, K. Myny, J. Genoe, and P. Heremans: Appl. Phys. Lett. **91** (2007) 103508.

21) B. Lucasa, A. E. Amrania, and A. Molitona: Mol. Cryst. Liq. Cryst. **485** (2008) 955.

22) X. Liua, G. Dong, D. Zhao, Y. Wang, L. Duan, L. Wang, and Y. Qiu: Org. Electron. **13** (2012) 2917.

23) B. Yao, W. Lv, D. Chen, G. Fan, M. Zhou, and Y. Peng: Appl. Phys. Lett. **101** (2012) 163301.

24) C. B. Park: IEEE Electron Device Lett. **33** (2012) 1765.

25) S. Okur and F. Yakuphanoglu: Sens. Actuators A **149** (2009) 241.

26) A. El Amrani, B. Lucas, and B. Ratier: Synth. Met. **161** (2012) 2566.

27) F. Yakuphanoglua and W. A. Farooq: Synth. Met. **161** (2011) 132.

28) B. Lucas, A. El Amrani, M. Chakaroun, B. Ratier, R. Antony, and A. Moliton: Thin Solid Films **517** (2009) 6280.

29) J.-M. Choi, J. Lee, D. K. Hwang, J. H. Kim, S. Im: Appl. Phys. Lett. **88** (2006) 043508.

30) A. El Amrani, B. Lucas, and A. Moliton: Eur. Phys.: J. Appl. Phys. **41** (2008) 19.

31) M. Murakami, K. Ohkubo, T. Nanjo, K. Souma, N. Suzuki, and S. Fukuzumi: ChemPhysChem **11** (2010) 2594.

32) S. M. Sze and K. K. Ng: *Physics of Semiconductor Devices* (Wiley, New York, 2007) 3rd ed., p. 306.

33) M. C. Hamilton, S. Martin, and J. Kanicki: IEEE Trans. Electron Devices **51** (2004) 877.

34) H. Sakai, K. Konno, and H. Murata: Appl. Phys. Lett. **94** (2009) 073304.

Figure captions

Fig. 1. (Color online) (a) Device structure of phototransistor, (b) chemical structures of pentacene and DPA-CM and (c) equivalent circuit of double-layer gate dielectric capacitor.

Fig. 2. (a) Output and (b) transfer characteristics of phototransistor under dark.

Fig. 3. (Color online) (a) Transfer characteristics of phototransistor under dark, UV light, and after turning off UV light, (b) R versus V_G under UV light intensity of 2.54 mW/cm^2 and (c) dependence of R on UV light intensity at different V_G.

Fig. 4. (Color online) (a) Transfer characteristics of transistor without DPA-CM under UV light. Device was characterized under UV light intensity of 2.54 mW/cm^2. (b) UV-VIS absorption spectra of 30-nm-thick penatacene and 260-nm-thick PMMA:DPA-CM.

Fig. 5. (Color online) (a) Device structure, (b) current versus UV light intensity and (c) change in R as function of UV light intensity of photoactive dielectric device. Device area is 4.95 mm^2.

Fig. 6. (Color online) Proposed operating model of phototransistor under (a) dark and (b) UV light.

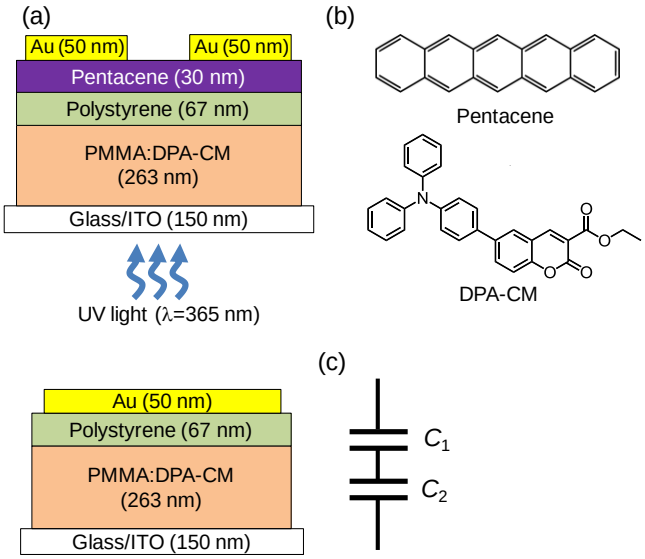

Fig. 1.

Dao *et al*.

Jpn. J. Appl. Phys.

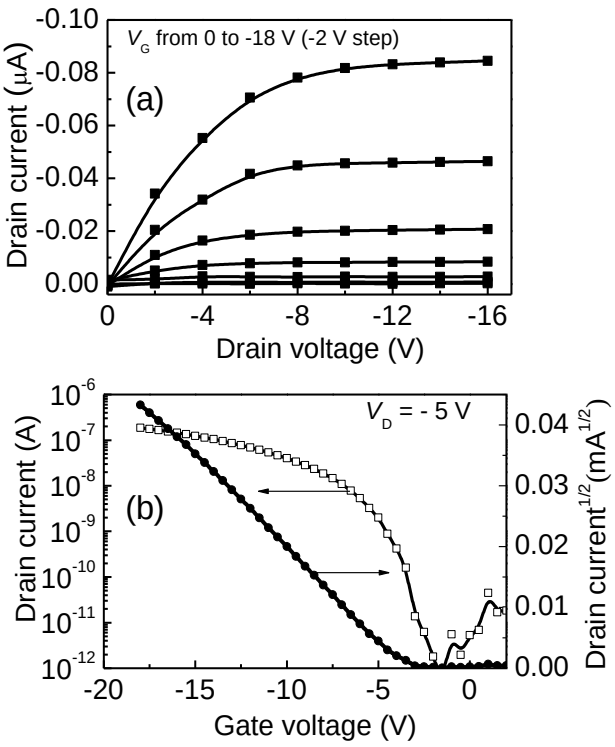

Fig. 2.

Dao *et al*.

Jpn. J. Appl. Phys.

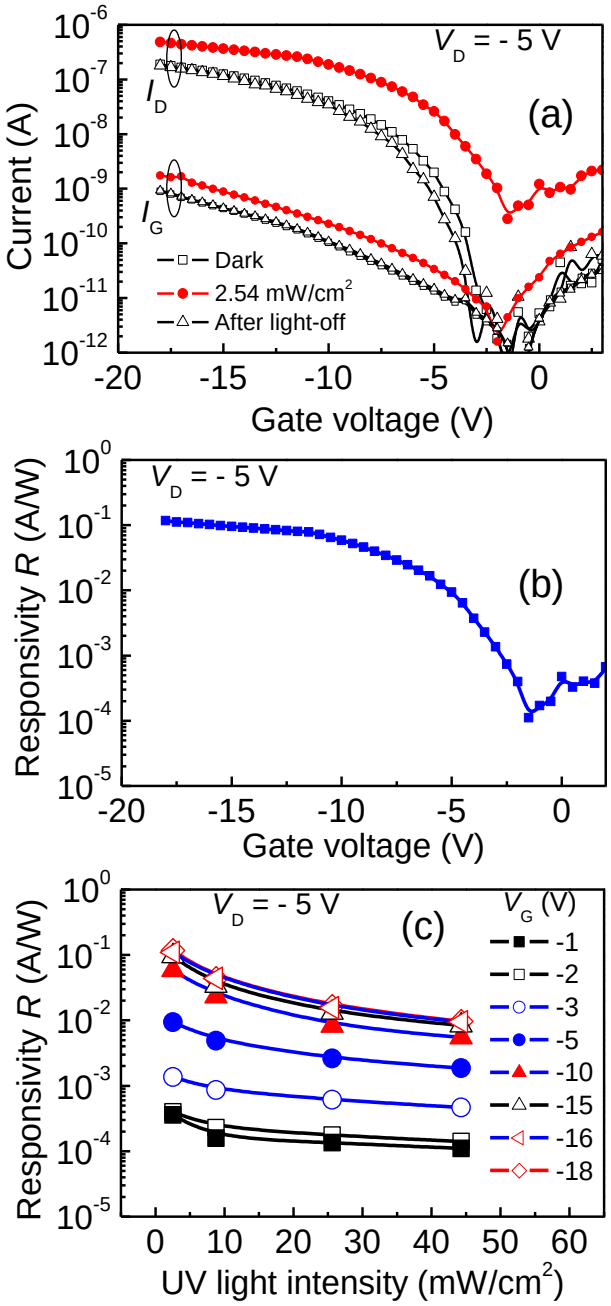

Fig. 3.

Dao *et al*.

Jpn. J. Appl. Phys.

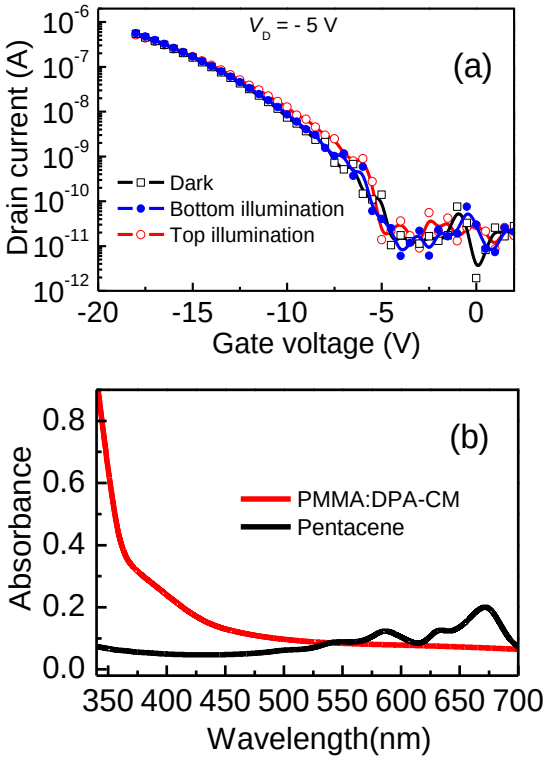

Fig. 4.

Dao *et al*.

Jpn. J. Appl. Phys.

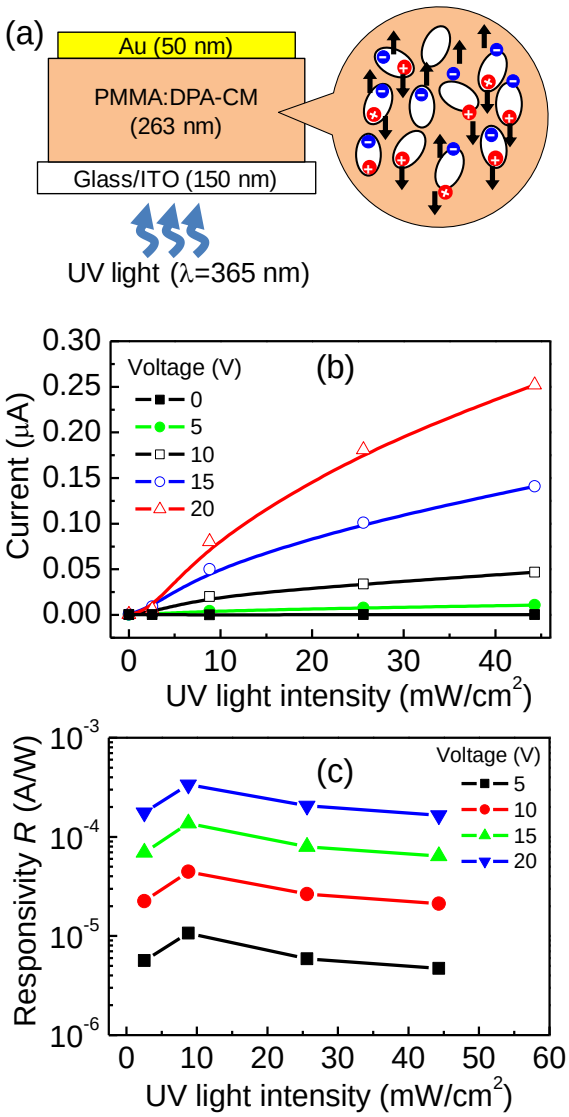

Fig. 5.

Dao *et al*.

Jpn. J. Appl. Phys.

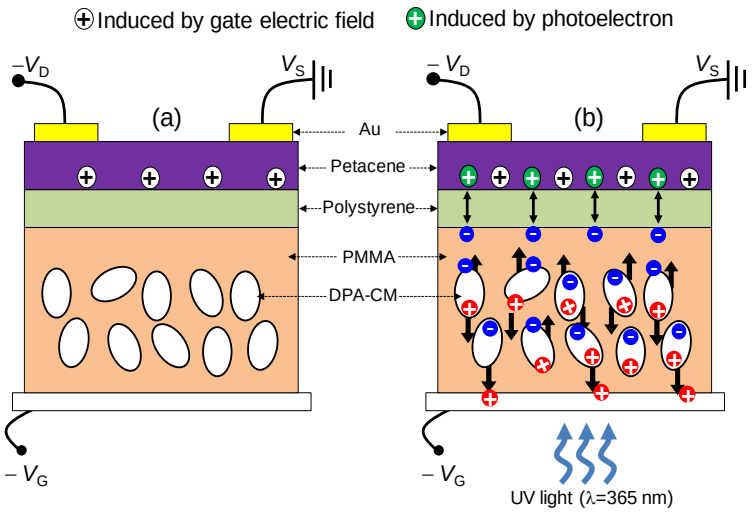

Fig. 6.

Dao *et al*.

Jpn. J. Appl. Phys.